

# $\alpha$ -Mangostin, a xanthone from mangosteen fruit, promotes cell cycle arrest in prostate cancer and decreases xenograft tumor growth

Jeremy J. Johnson\*, Sakina M. Petiwala, Deeba N. Syed<sup>1</sup>, John T. Rasmussen, Vaqar M. Adhami<sup>1</sup>, Imtiaz A. Siddiqui<sup>1</sup>, Amanda M. Kohl<sup>1</sup> and Hasan Mukhtar<sup>1</sup>

Department of Pharmacy Practice, University of Illinois at Chicago College of Pharmacy, 833 South Wood Street, Chicago, IL 60612-7230, USA and <sup>1</sup>Department of Dermatology, University of Wisconsin School of Medicine and Public Health, Madison, WI 53706, USA

\*To whom correspondence should be addressed. Tel: +1 312 996 4368;  
Fax: +1 312 996 0379;  
Email: jjjohn@uic.edu

**There is a need to characterize promising dietary agents for chemoprevention and therapy of prostate cancer (PCa). We examined the anticancer effect of  $\alpha$ -mangostin, derived from the mangosteen fruit, in human PCa cells and its role in targeting cell cycle-related proteins involved in prostate carcinogenesis. Using an 3-(4,5-dimethylthiazol-2-yl)-2,5-diphenyltetrazolium bromide assay, we found that  $\alpha$ -mangostin significantly decreases PCa cell viability in a dose-dependent manner. Further analysis using flow cytometry identified cell cycle arrest along with apoptosis. To establish a more precise mechanism of action, we performed a cell free biochemical kinase assay against multiple cyclins/cyclin-dependent kinases (CDKs) involved in cell cycle progression; the most significant inhibition in the cell free-based assays was CDK4, a critical component of the G1 phase. Through molecular modeling, we evaluated  $\alpha$ -mangostin against the adenosine triphosphate-binding pocket of CDK4 and propose three possible orientations that may result in CDK4 inhibition. We then performed an *in vivo* animal study to evaluate the ability of  $\alpha$ -mangostin to suppress tumor growth. Athymic nude mice were implanted with 22Rv1 cells and treated with vehicle or  $\alpha$ -mangostin (100 mg/kg) by oral gavage. At the conclusion of the study, mice in the control cohort had a tumor volume of 1190 mm<sup>3</sup>, while the treatment group had a tumor volume of 410 mm<sup>3</sup> ( $P < 0.01$ ). The ability of  $\alpha$ -mangostin to inhibit PCa *in vitro* and *in vivo* suggests  $\alpha$ -mangostin may be a novel agent for the management of PCa.**

## Introduction

Of all cancers, prostate cancer (PCa) is ideal for evaluating chemopreventive agents for four main reasons: (i) it is typically diagnosed in men >50 years old, (ii) its high latency period, (iii) upon initial diagnosis patients often undergo 'watchful waiting' and (iv) it could be targeted at various stages of disease development. For these reasons, even a slight delay in the pathogenesis of PCa with chemoprevention has the potential to result in a substantial reduction in the incidence of PCa as well as significantly increase the quality of life in these patients. Over the last several decades, epidemiological, human migratory studies, preclinical and even early phase clinical trials have suggested that selected dietary constituents may offer a protective effect in reducing the incidence of multiple cancers, including cancer of the prostate (1–3). Given the potential that some of these phytochemicals have shown it is essential to further identify and develop promising new agents in the hope of creating a broad spectrum of cancer chemopreventive agents that could be used alone or in combination.

The purple mangosteen (*Garcinia mangostana*) is a slow growing tropical tree native to India, Myanmar, Malaysia, Philippines, Sri

**Abbreviations:** ATP, adenosine triphosphate; CDK, cyclin-dependent kinase; MTT, 3-(4,5-dimethylthiazol-2-yl)-2,5-diphenyltetrazolium bromide; PCa, prostate cancer; PrEC, prostate epithelial cells.

Lanka and Thailand and is reported to reach heights of 6–25 m (20–80 ft) (4,5). The purple mangosteen (here after referred to as mangosteen) is related to several other fruits including button mangosteen (*G. prainiana*) and the lemon drop mangosteen (*G. madruno*). For clarification, the mangosteen is unrelated to the mango (*Mangifera* spp.). A class of compounds known as xanthenes have been isolated from the mangosteen with well over 60 different xanthenes isolated from the fruit, leaves, bark and roots (4,5). A variety of health-promoting attributes have been associated with the mangosteen, which include antiinflammatory (6–8), antibacterial activity (9), cardioprotective (10,11) and antioxidant activity (12–16). Of all the xanthenes,  $\alpha$ -mangostin (1,3,6-Trihydroxy-7-methoxy-2,8-bis(3-methyl-2-butenyl)-9H-xanthen-9-one) has been identified as the most abundant xanthone and as a result has received the most attention for its health-promoting properties.

In preclinical settings, crude mangosteen extract containing  $\alpha$ -mangostin and  $\gamma$ -mangostin was shown to decrease preneoplastic lesions in the colon of rat exposed to dimethylhydrazine (17). A significant suppression in the development of aberrant crypt foci was evident in rats administered  $\alpha$ -mangostin as a part of their daily diet. A significant reduction in dysplastic foci and  $\beta$ -catenin accumulated crypts was also observed ( $P < 0.05$ ). Recently,  $\alpha$ -mangostin has been shown to inhibit matrix metalloproteinase-2/9 through the c-jun N-terminal kinase (JNK) signaling pathway in PC3 cells (18).

We hypothesized that a highly purified form of  $\alpha$ -mangostin (>95%) may offer cancer chemopreventive and/or chemotherapeutic effects against PCa. For our study, we evaluated  $\alpha$ -mangostin for its ability to inhibit PCa cell growth, induce apoptosis, inhibit deregulated kinases in PCa and suppress tumor growth in 22Rv1 xenograft mice.

## Materials and methods

$\alpha$ -Mangostin (Xanomax 95<sup>TM</sup>, >95%) was obtained from Avesthagen (Chatsworth, CA), 3,3'-Diindolylmethane (>98%), Genistein (>98%), Epigallocatechin 3-gallate (>97%) was obtained from Sigma (St Louis, MO), 5-(N-(4-Methylphenyl)amino)-2-methyl-4,7-dioxobenzothiazole (CDK 4 Inhibitor;  $\geq 95\%$ ) and *trans*-4-((6-(ethylamino)-2-((1-(phenylmethyl)-1H-indol-5-yl)amino)-4-pyrimidinyl)amino)-cyclohexanol (CDK4/6 Inhibitor;  $\geq 95\%$ ) were obtained from EMD Chemicals (Gibbstown, NJ). All antibodies for western blot analysis were obtained from Cell Signaling Technology (Danvers, MA). Protein assay kit was obtained from Pierce (Rockford, IL). APO-DIRECT<sup>TM</sup> kit was obtained from Phoenix Flow Systems (San Diego CA). Cleaved caspase-3 kit was obtained from Cell Signaling Technology. General caspase inhibitor (z-vad-fmk) was obtained from R&D Systems (Minneapolis, MN).

### Cell culture and treatment

LNCaP, PC3, DU145 and 22Rv1 cells were obtained from American Type Culture Collection (Manassas, VA). These cells were cultured in RPMI (LNCaP, PC3 and 22Rv1) or DMEM (DU145) supplemented with 10% fetal bovine serum and 1% penicillin/streptomycin. Human normal prostate epithelial cells (PrEC) were obtained from Lonza (Basel, Switzerland) and grown according to the manufacturer's instructions. All cells were maintained under standard cell culture conditions as described previously (19).

### Cell viability

Cell viability was determined after 48 h by 3-(4,5-dimethylthiazol-2-yl)-2,5-diphenyltetrazolium bromide (MTT) assay as described previously (20).

### Flow cytometry

The APO-DIRECT<sup>TM</sup> kit (Phoenix Flow Systems) was used for measuring apoptosis and cell cycle of treated cells by flow cytometry (21). Briefly, PC3 and 22Rv1 cells were 50–60% confluent and were serum depleted (i.e. 0.1%) for 36 h to promote cell synchronization. Cells were then treated with complete media containing  $\alpha$ -mangostin for 24 and 48 h. The kit was followed per protocol directions.

### Colony formation

22Rv1 and PC3 cells were seeded in six well plates at a concentration of 1000 cells per well and incubated for 48 h. Cells were then treated with increasing

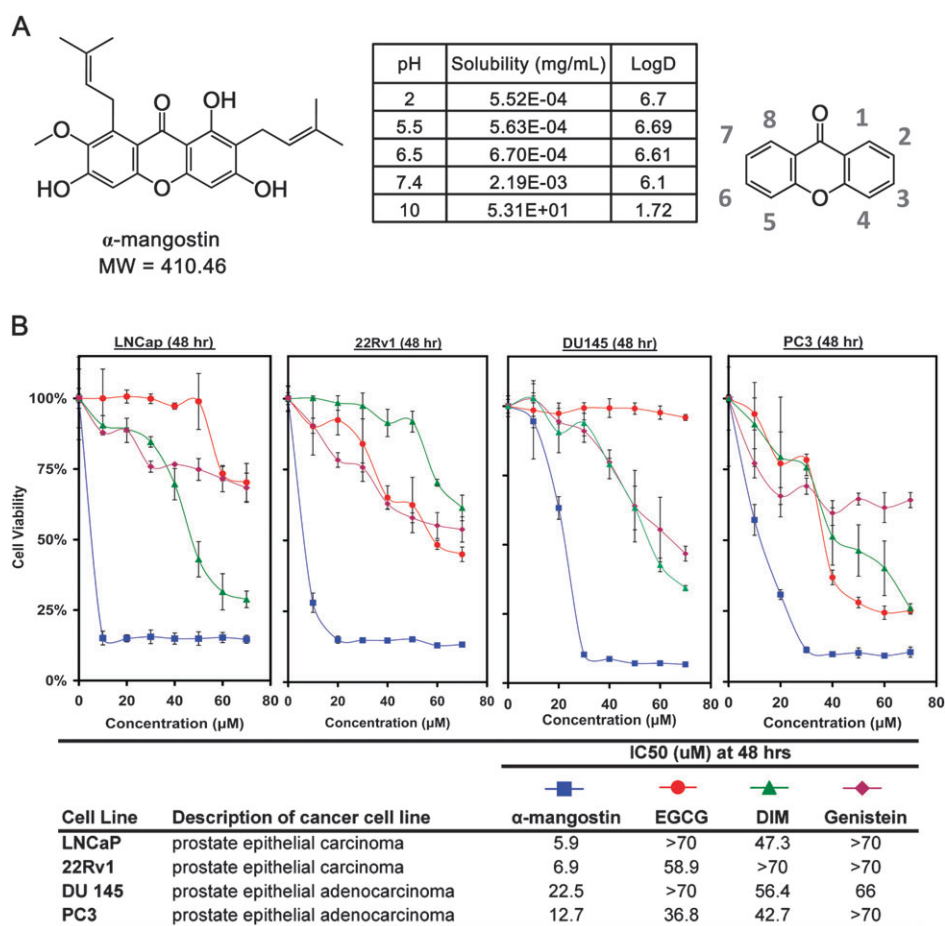


**Fig. 1.** (A) Chemical structure of  $\alpha$ -mangostin and nomenclature of a xanthone. (B) Cell viability assay was performed treating cells with  $\alpha$ -mangostin, Epigallocatechin 3-gallate, Genistein and 3,3'-Diindolylmethane up to 70  $\mu$ M against four PCa cell lines (LNCaP, 22Rv1, DU145 and PC3) for 48 h. Data points are represented by the average of three values with standard deviation and representative of two different experiments.

concentrations of  $\alpha$ -mangostin (2.5–20  $\mu$ M). Fresh media containing  $\alpha$ -mangostin was replaced every 3–4 days until the conclusion of the study, which was 15 days after initiating the study. Media was removed and wells were briefly rinsed with 1X phosphate-buffered saline and removed. Colonies were then stained with crystal violet in triplicate and colonies were counted visually.

#### Western blots

After 24 h of cell growth, the complete media was removed and replaced with media containing  $\alpha$ -mangostin with the appropriate assay concentrations for the whole-cell lysates as depicted in figures. Cell lysates were prepared as previously described (20).

#### Kinase assay

$\alpha$ -Mangostin was diluted into assay mixture where concentrations of  $\alpha$ -mangostin ranged from 1 to 10  $\mu$ M of  $\alpha$ -mangostin to determine inhibition of JNK1, JNK2, JNK3, CyclinA1/CDK2, CyclinA2/CDK2, CyclinD1/CDK4, CyclinD3/CDK6 (Kinexus, Vancouver, British Columbia, Canada). The IC<sub>50</sub> was determined for  $\alpha$ -mangostin against CyclinD1/CDK4 with six dilutions ranging from 2.5 to 15  $\mu$ M. The assay was initiated by the addition of [<sup>33</sup>P]-ATP and the reaction mixture incubated at room temperature for 20–40 min. After the incubation period, the assay was terminated by spotting 10  $\mu$ l of the reaction mixture onto multiscreen phosphocellulose P81 plate. The multiscreen phosphocellulose P81 plate was washed three times for ~15 min each in a 1% phosphoric acid solution. The radioactivity on the P81 plate was counted in the presence of scintillation fluid in a Trilux scintillation counter. Protein kinase-specific activity of [<sup>33</sup>P]-ATP incorporated per minute per sample was determined. A total counts per minute for each reaction sample was determined for blanks (without substrate), control (without  $\alpha$ -mangostin) and samples (with  $\alpha$ -mangostin). The corrected activity for control samples (i.e. without  $\alpha$ -mangostin) represented 100% kinase activity and was used to determine the percent of kinase activity.

#### *In vivo* 22Rv1 tumor xenograft model

Athymic (nu/nu) male nude mice (Harlan Laboratory, Madison, WI) 7–8 weeks old were housed under pathogen-free conditions with a 12 h light/12 h dark schedule and fed with an autoclaved AIN-76A diet ad libitum as described previously (21). 22Rv1 cells were used for determining the *in vivo* effects of  $\alpha$ -mangostin based on the fact that these cells form rapid and reproducible tumors in nude mice with tumor xenografts established as described previously (21). Fourteen animals were randomly divided into two groups, with seven animals in each group. The animals in group 1 received vehicle (100  $\mu$ l) by oral gavage and served as control. The animals in group 2 received  $\alpha$ -mangostin (100 mg/kg) by oral gavage five times weekly. Body weights were recorded once weekly throughout the study. All procedures conducted were in accordance with the guidelines for the use and care of laboratory animals.

#### Statistical analysis

All statistical analysis was performed by using VassarStats software. Data are expressed as mean with standard deviation for all groups. Statistical significance of differences in all measurements between control and treated groups was determined by one-way analysis of variance followed by Tukey's HSD test for multiple comparisons. Student's paired *t* test was used for pair wise group comparisons, as needed. All statistical tests were two-sided, and *P* < 0.05 was considered statistically significant.

## Results

#### $\alpha$ -Mangostin decreases PCa cell viability

PCa cells (LNCaP, 22Rv1, DU145 and PC3) were treated for 48 h with  $\alpha$ -mangostin, Epigallocatechin 3-gallate, 3,3'-Diindolylmethane, and genistein and evaluated for decreasing PCa cell viability using the MTT assay. These cells were selected based on their

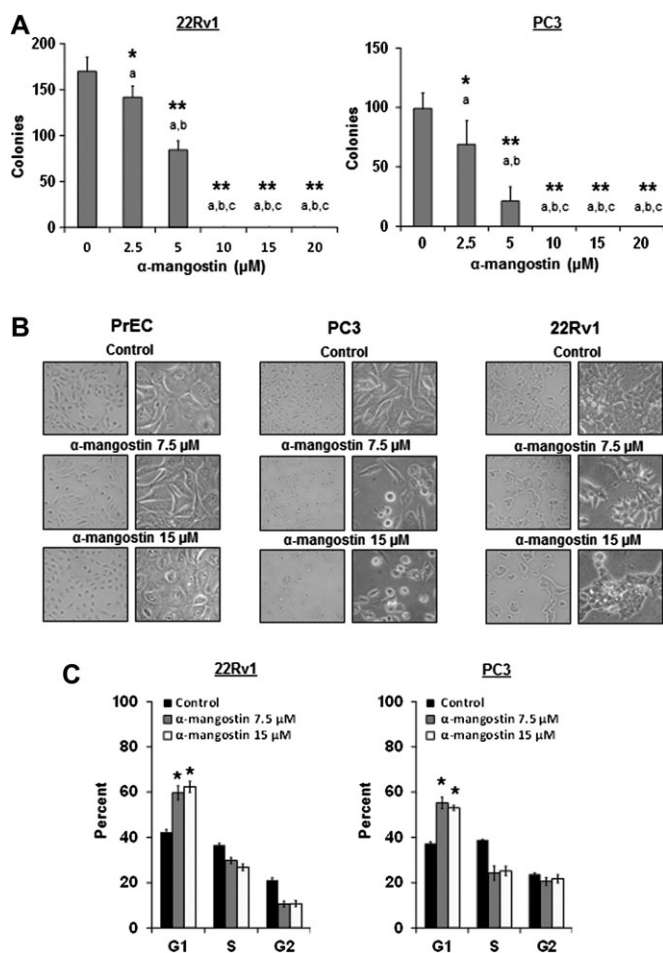


**Fig. 2.** (A) Colony formation was performed using 22Rv1 and PC3 cells. For colony formation, cells were plated at ~1000 cells per well and incubated for 48 h. After 48 h, media was replaced with fresh media containing  $\alpha$ -mangostin and was repeated every 3–4 days until completion of the experiment. Statistical analysis performed using VassarStats software by one way analysis of variance and the Tukey test. ‘a’ versus control, ‘b’ versus 2.5  $\mu$ M, ‘c’ versus 5  $\mu$ M. (B) Phase contrast microscopic images (10x and 40x) of PrECs, PC3 and 22Rv1 cells with control and  $\alpha$ -mangostin-treated cells (7.5 and 15  $\mu$ M) are shown. Cells were treated for 48 h. (C) Cell cycle analysis was performed per manufacturer’s protocol using synchronized PC3 cells. Cells were synchronized for 36 h and then treated with  $\alpha$ -mangostin for 24 h. These experiments were performed in triplicate and are represented by the mean along with standard deviation. These results were consistent with 22Rv1 cells treated with  $\alpha$ -mangostin. Statistical analysis was performed using VassarStats software by one way analysis of variance and statistical significance was performed by the Tukey test with \* $P$  < 0.01 and \*\* $P$  < 0.001.

response to androgens with LNCaP being androgen dependent, 22Rv1 being androgen independent but androgen sensitive and both DU145 and PC3 being androgen independent. The  $IC_{50}$  of  $\alpha$ -mangostin was calculated to be 5.9, 6.9, 22.5 and 12.7  $\mu$ M in all four cell lines (LNCaP, 22Rv1, DU145 and PC3, respectively) (Figure 1B).

*$\alpha$ -Mangostin inhibits colony formation in PCa cells*

Next, we evaluated  $\alpha$ -mangostin for decreasing the clonogenic potential of 22Rv1 and PC3 cells. 22Rv1 and PC3 cells were seeded at a concentration of 1000 cells per well and treated with increasing concentrations of  $\alpha$ -mangostin every 3–4 days. We observed a statistically significant ( $P$  < 0.01) decrease in colony formation at doses of 2.5  $\mu$ M in both cell lines and a complete inhibition of colony formation at 10  $\mu$ M after 12–14 days (Figure 2A).  $\alpha$ -Mangostin was not found to inhibit normal human PrEC using  $\alpha$ -mangostin at 7.5 and 15  $\mu$ M after 48 h as shown in Figure 2B. These cells were also

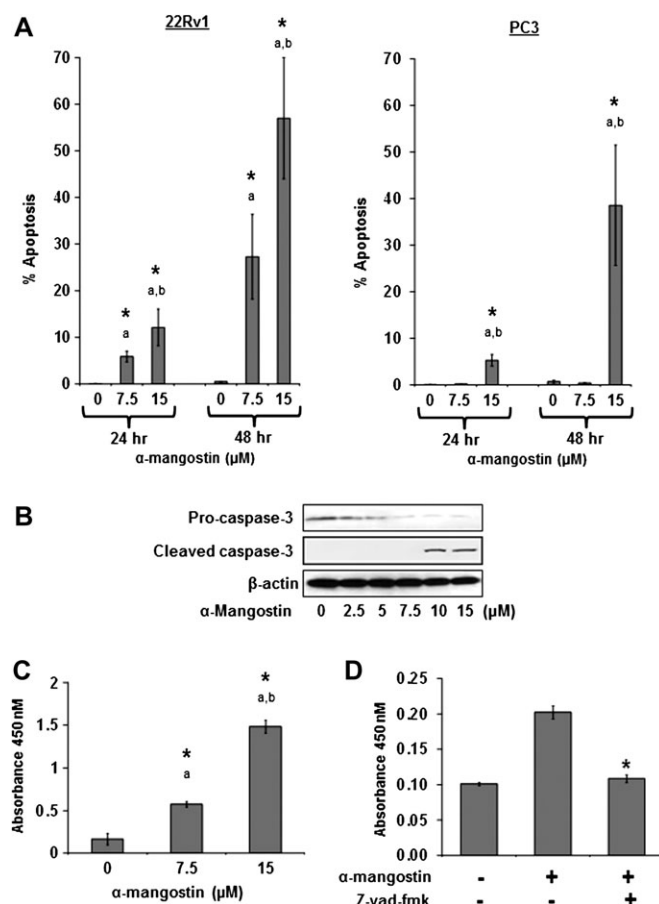


**Fig. 3.** (A) PC3 and 22Rv1 cells were treated with  $\alpha$ -mangostin for 24 and 48 h and evaluated for apoptosis per manufacturer’s protocol. Cells were synchronized for 36 h and then treated with  $\alpha$ -mangostin for 24 h. These experiments were performed in triplicate and are represented by the mean along with standard deviation. Statistical analysis was performed using VassarStats software by one way analysis of variance and statistical significance was performed by the Tukey test with \* $P$  < 0.01. ‘a’ versus control, ‘b’ versus 7.5  $\mu$ M. (B) 22Rv1 cells were grown to 60–70% confluence and treated with  $\alpha$ -mangostin up to 24 h and whole cell lysates were prepared as described in Materials and methods. Seventy micrograms of protein was subjected to sodium dodecyl sulfate–polyacrylamide gel electrophoresis followed by western blot analysis and chemiluminescence detection. Equal loading of protein was confirmed by stripping the immunoblot and reprobing it for  $\beta$ -actin. (C) 22Rv1 cells were treated with  $\alpha$ -mangostin for 24 h and whole cell lysates were collected to evaluate for active caspase-3 protein by enzyme-linked immunosorbent assay. These experiments were performed in triplicate and are represented by the mean along with standard deviation. Statistical analysis was performed using VassarStats software by one way analysis of variance and statistical significance was performed by the Tukey test with \* $P$  < 0.01. ‘a’ versus control, ‘b’ versus 7.5  $\mu$ M. (D) 22Rv1 cells were treated with general caspase inhibitor z-vad-fmk (100  $\mu$ M) for 2 h and then treated with  $\alpha$ -mangostin for 18 h. Whole cell lysates were collected to evaluate for active caspase-3 protein by enzyme-linked immunosorbent assay. These experiments were performed in triplicate and are represented by the mean along with standard deviation.

evaluated for viability using MTT at 5, 10, 15, 20, 25, 30 and 35  $\mu$ M  $\alpha$ -mangostin that had 104.7% ( $\pm$ 5.2), 104.6% ( $\pm$ 1.6), 103.7% ( $\pm$ 3.0), 103.3% ( $\pm$ 9.7), 58.3% ( $\pm$ 7.2), 51.5% ( $\pm$ 5.2), 51.1% ( $\pm$ 5.2) cell viability compared with control PrEC.

*$\alpha$ -Mangostin induces G<sub>1</sub> cell cycle arrest in PCa cells*

22Rv1 and PC3 cells treated with  $\alpha$ -mangostin for 24 h were evaluated by flow cytometry for cell cycle arrest.  $\alpha$ -Mangostin resulted in a statistically significant ( $P$  < 0.01) higher number of cells in G<sub>1</sub>. As summarized in Figure 2C, after 24 h, the number of 22Rv1 cells in G<sub>1</sub>

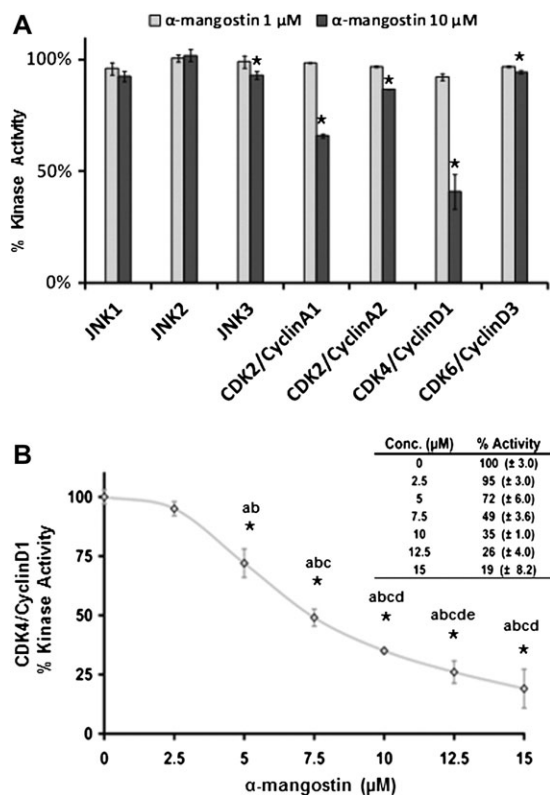


**Fig. 4.** (A) Cell free biochemical-based kinase assay was evaluated ( $\alpha$ -mangostin 1 and 10  $\mu$ M) against JNK 1/2/3, CyclinA1/CDK2, cyclinA2/CDK2, CyclinD1/CDK4 and CyclinD3/CDK6. Statistical analysis was performed using VassarStats software by one way analysis of variance and statistical significance was performed by the Tukey test with  $*P < 0.01$ . (B) Cell free biochemical kinase assay established the  $IC_{50}$  of  $\alpha$ -mangostin against CyclinD1/CDK4. Data points are represented by the average of three values with standard deviation. As a positive control staurosporine, a potent microbial-derived general kinase inhibitor was used (data not shown). Statistical analysis was performed using VassarStats software by one way analysis of variance and statistical significance was performed by the Tukey test with  $*P < 0.01$ . 'a' versus control, 'b' versus 2.5  $\mu$ M, 'c' versus 5  $\mu$ M, 'd' versus 7.5  $\mu$ M, 'e' versus 10  $\mu$ M.

phase increased from the control ( $42.3\% \pm 1.19$ ) compared with 7.5  $\mu$ M  $\alpha$ -mangostin ( $59.6\% \pm 3.09$ ;  $P < 0.01$ ) and 15  $\mu$ M  $\alpha$ -mangostin ( $62.4\% \pm 2.4$ ;  $P < 0.01$ ). In addition, the number of PC3 cells in  $G_1$  increased from the control ( $37.35\% \pm 0.77$ ) compared with 7.5  $\mu$ M  $\alpha$ -mangostin ( $55.24\% \pm 2.51$ ;  $P < 0.01$ ) and 15  $\mu$ M  $\alpha$ -mangostin ( $53.06\% \pm 1.09$ ;  $P < 0.01$ ). These results suggest that an inhibition in cell viability may be associated with the induction of cell cycle arrest.

#### $\alpha$ -Mangostin induces apoptosis in PCa cells

Using flow cytometry, we evaluated PC3 and 22Rv1 cells treated with  $\alpha$ -mangostin for apoptosis by end labeling DNA fragments with fluorescently tagged deoxyuridine triphosphate nucleotides (F-dUTP). After 48 h, treatment with  $\alpha$ -mangostin (15  $\mu$ M) resulted in  $38.56\% \pm 12.93$  ( $P < 0.01$ ) of the cells undergoing apoptosis (Figure 3A). We also observed similar results with 22Rv1 cells treated with  $\alpha$ -mangostin  $57.0\% \pm 26.9$  cells undergoing apoptosis at 15  $\mu$ M, respectively ( $P < 0.01$ ). By western blot, we observed a decrease in pro-caspase-3 and an increase in the active form of caspase-3 in 22Rv1 cells (Figure 3B) allowing for a qualitative confirmation that apoptosis was occurring. To accurately quantify the extent of caspase-3 activation, we performed an enzyme-linked immunosorbent assay to detect activated caspase-3 in 22Rv1 cells treated with  $\alpha$ -mangostin for 24 h and identified an increase in the cleaved form of caspase-3 (Figure 3C) at 7.5 and 15  $\mu$ M by 345 and 894%, respectively, compared with control cells. When PCa cells were treated with a general caspase inhibitor (Z-VAD-FMK) prior to the

treatment of  $\alpha$ -mangostin, the cleavage of caspase-3 to its active form was inhibited (Figure 3D).

#### $\alpha$ -Mangostin inhibits kinases in a cell free biochemical based-assay

Using a cell free-based kinase assay, we evaluated  $\alpha$ -mangostin (1 and 10  $\mu$ M) for its ability to inhibit several kinases that included the JNK and cyclin/cyclin-dependent kinase (CDK) proteins (Figure 4A). A significant inhibition ( $P < 0.01$ ) was observed at the following cyclins/CDKs: cyclinA1/CDK2 ( $34.2\% \pm 0.1$ ) and cyclinA2/CDK2 ( $13.2\% \pm 0.4$ ), cyclinD1/CDK4 ( $59.2 \pm 1.4$ ) and cyclinD3/CDK6 ( $5.5\% \pm 0.3$ ) with 10  $\mu$ M  $\alpha$ -mangostin. No direct inhibition of kinase activity was observed with treatment of JNK1 and JNK2 at either 1 or 10  $\mu$ M. A slight but significant decrease ( $P < 0.01$ ) in kinase activity at 10  $\mu$ M was observed with JNK3 ( $7\% \pm 2.8$ ). The greatest decrease in kinase activity by  $\alpha$ -mangostin was observed with cyclinD1/CDK4. As a result, cyclinD1/CDK4 was evaluated in further studies. The  $EC_{50}$  of  $\alpha$ -mangostin and cyclinD1/CDK4 was determined to be 7.4  $\mu$ M (Figure 4B).

#### $\alpha$ -Mangostin modulates proteins involved in cell cycle in PCa cells

Next, we assessed the effect of  $\alpha$ -mangostin to inhibit proteins upstream of CDK4 that included the INK proteins (p15 INK4B, p16 INK4A), p27 Kip1 and CDK4 (Figure 5A) in 22Rv1 cells. An increase in p27 Kip1 was observed in cells treated with  $\alpha$ -mangostin, however no effect was observed on p15 INK4B, p16 INK4A or CDK4. A decrease in protein expression was observed with both cyclins D1 and D3. Next, we evaluated the downstream targets of CDK4, specifically the phosphorylation sites of retinoblastoma protein. A dose-dependent decrease in the levels of phosphorylated retinoblastoma protein at residues Ser780, Ser795 and Ser807/811 was observed (Figure 5B). The retinoblastoma protein has been shown to regulate the expression of cyclin E and we were able to observe a decrease in protein expression of cyclin E consistent with the notion that  $\alpha$ -mangostin decreases the phosphorylated retinoblastoma protein.

#### CDK4 inhibitors decrease cell viability

Using an MTT cell viability assay, 22Rv1 cells were treated with a CDK4 inhibitor and a CDK4/6 inhibitor for 48 h (Figure 5C). Interestingly, we found that the CDK4 inhibitor increased the cell viability at a lower dose of 2.5  $\mu$ M to  $134.9\% \pm 0.9$  followed by a decrease to  $41.2\% \pm 4.5$  when treated with 5  $\mu$ M with an estimated  $IC_{50}$  of 4.4  $\mu$ M. Similarly, we found that a CDK4/6 inhibitor increased the cellular viability at 2.5–10  $\mu$ M followed by a decrease to  $23.7\% \pm 1.3$  at 20  $\mu$ M with an estimated  $IC_{50}$  of 16.7  $\mu$ M. These stimulatory effects were not observed when cells were treated with  $\alpha$ -mangostin. In addition, we performed *in silico* docking using the CDK4 and CDK4/6 inhibitors with the ATP binding pocket of CDK4. Using AutoDock 4.2, the CDK4 inhibitor was found to be positioned with the methoxy groups going into the binding pocket first, possibly owing to their hydrophobic properties. The cyclohexyl-OH functional group on the CDK4/6 inhibitor was found to position itself deep into the binding pocket with the phenyl group positioned out into solution.

#### $\alpha$ -Mangostin/CDK 4-binding hypothesis by molecular modeling

Next, through *in silico* docking using AutoDock 4.2, we evaluated 30 possible binding configurations of  $\alpha$ -mangostin with the binding pocket of CDK4 to generate a binding hypothesis. The structure of CDK4 in the present study is from the crystal structure of cyclinD1/CDK4 and was used for molecular modeling studies (22). From the 30 different arrangements, several clusters were generated, and we have presented the three most common clusters designating them cluster 1 (yellow), cluster 2 (green) and cluster 3 (gold) (Figure 5D). In cluster 1, the isoprenyl group at the second carbon of  $\alpha$ -mangostin was found to position itself deep within the hydrophobic ATP-binding pocket of CDK4 positioning itself near the phenylalanine-93. In clusters 2 and 3, the opposite end of  $\alpha$ -mangostin (i.e. carbons 5–8)

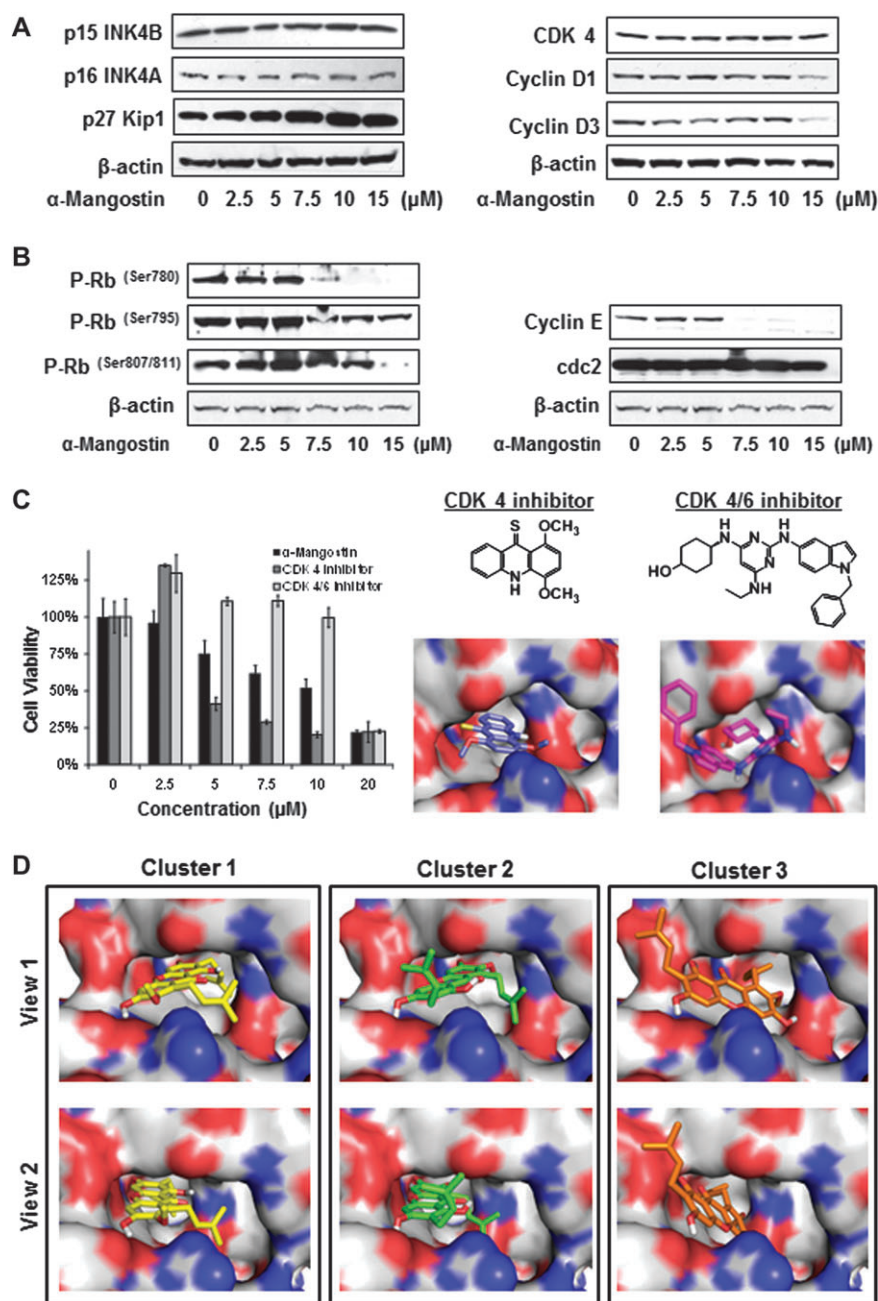


**Fig. 5.** (A and B) 22Rv1 cells were grown to 60–70% confluence and treated with  $\alpha$ -mangostin up to 24 h and whole cell lysates were prepared as described in Materials and methods. Forty micrograms of protein was subjected to sodium dodecyl sulfate–polyacrylamide gel electrophoresis followed by western blot analysis and chemiluminescence detection. Equal loading of protein was confirmed by stripping the immunoblot and reprobing it for  $\beta$ -actin. (C) Cell viability assay was performed treating cells with 5-(N-(4-Methylphenyl)amino)-2-methyl-4,7-dioxobenzothiazole (CDK4 Inhibitor) and *trans*-4-((6-ethylamino)-2-((1-(phenylmethyl)-1H-indol-5-yl)amino)-4-pyrimidinyl)amino)-cyclohexanol (CDK6 Inhibitor) up to 20  $\mu$ M against 22Rv1 cells for 48 h. Data points are represented by the average of three values with bars representing standard deviation. Molecular modeling of CDK4 interacting with CDK4 and CDK4/6 inhibitor shown at the ATP binding site and was analyzed using Autodock 4.2 with surface structure images created using PyMOL. (D) Molecular modeling of CDK4 interacting with  $\alpha$ -mangostin is shown at the ATP binding site and was analyzed using Autodock 4.2 with surface structure images created using PyMOL (protein colors: gray = carbon, blue = nitrogen and red = oxygen). Thirty different binding configurations were created with the three highest scoring configurations presented.  $\alpha$ -Mangostin is presented as a different color in each configuration: cluster 1 (yellow), cluster 2 (green) and cluster 3 (gold).

went into the binding pocket first. In the second and third cluster, there appears to be limitations in that they do not fill the binding pocket of CDK4 as well as cluster 1 making them less favored. In each of the different cluster arrangements, the hydrogen bonding could occur with the three hydroxyl groups on  $\alpha$ -mangostin at aspartate-99, arginine-101 and threonine-102. The carbonyl group did not interact with any amino acids but rather seemed to stabilize the hydroxyl group at the first carbon of  $\alpha$ -mangostin.

*$\alpha$ -Mangostin inhibits the growth of human prostate carcinoma 22Rv1 cells in athymic nude mice*

Athymic nude mice were implanted with 22Rv1 cells and divided into two cohorts receiving vehicle or  $\alpha$ -mangostin (100 mg/kg). We found  $\alpha$ -mangostin was as tolerable as the vehicle throughout the experiment, this was evidenced by body weight measurements (Figure 6A). In the control cohort, tumors were measurable on day 14 while the cohort treatment with  $\alpha$ -mangostin at 100 mg/kg did not have

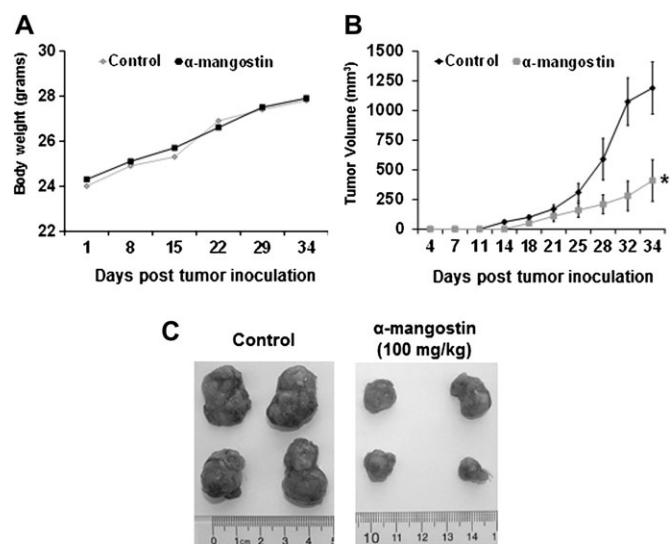


**Fig. 6.** (A) Body weights of athymic nude mice treated with  $\alpha$ -mangostin were measured one time weekly. (B) Fourteen animals were subcutaneously injected in each flank of the mouse with  $\sim 1.5 \times 10^6$  22Rv1 cells to initiate tumor growth. Twenty-four hours after cell implantation, the animals in each cohort received by oral gavage vehicle or  $\alpha$ -mangostin (100 mg/kg). The average tumor volume of control and  $\alpha$ -mangostin treated mice were plotted over days after tumor cell inoculation. Data points represent the mean of 14 tumors from seven mice; bars represent standard deviation of the mean,  $*P < 0.01$ . (C) Four representative tumors from each cohort at the end of the study are shown comparing control mice to mice treated with  $\alpha$ -mangostin.

measurable tumors until day 18 (Figure 6C). The average computed tumor volume was significantly inhibited in mice receiving  $\alpha$ -mangostin and can be visualized in Figure 6B. In the control group, the average tumor volume of 1190 mm<sup>3</sup> was reached on day 34 after tumor cell inoculation, whereas mice receiving  $\alpha$ -mangostin had an average tumor volume of 410 mm<sup>3</sup> (70 mg/kg). This represents a significant suppression in tumor growth by 65% ( $P < 0.01$ ), respectively, compared with control.

## Discussion

PCa is most often defined by a slow progression through well-defined stages beginning with hyperplasia through adenocarcinoma. This slow progression represents an important opportunity to either stop or delay the progression of this disease. One strategy to manage this progression is through chemoprevention using either dietary or synthetic agents that can delay, prevent or reverse the process of carcinogenesis. In our study, we observed  $\alpha$ -mangostin to promote cell cycle arrest by targeting CDK4 using a cell free kinase assay and confirmed the promotion of cell cycle arrest in PC3 and 22Rv1 cells. Furthermore,  $\alpha$ -mangostin promoted apoptosis through the activation of caspase-3 in 22Rv1 cells. Using athymic nude mice, 22Rv1 xenografts, we observed that the oral administration of  $\alpha$ -mangostin resulted in a 65% smaller tumor compared with vehicle-treated mice.

Ideally, new chemical entities that are being evaluated as an investigational drug should have little to no toxicity. Xanthones isolated from the pericarp of the mangosteen are not genotoxic in mutagenesis studies (23). In addition,  $\alpha$ -mangostin (10  $\mu$ M) was not found to be toxic to human peripheral blood lymphocytes even though identical treatment in leukemia cell lines lead to apoptosis (24). In our results, by MTT assay, we did not observe  $\alpha$ -mangostin to decrease cell viability of PrEC compared with PCa cells suggestive of selectivity. In two different cardioprotective studies,  $\alpha$ -mangostin was administered 200 mg/kg by oral gavage to rats for up to 8 days with no observable adverse effects in solid organ systems (10,11). In another study,  $\alpha$ -mangostin was tolerable with no observable adverse effects during a 5 weeks intervention with custom-blended food

pellets that contained 0.02 or 0.05%  $\alpha$ -mangostin in F344 rats (17). In addition, mangosteens that contain  $\alpha$ -mangostin are consumed by humans in the forms of juices (e.g. Xango®), dietary supplements standardized to  $\alpha$ -mangostin (e.g. Nature's Way® 80 mg  $\alpha$ -mangostin/capsule) and as a fruit. Investigators have shown that when rats are administered 40 mg/kg body wt of  $\alpha$ -mangostin in corn oil the maximum plasma concentration was 11.7  $\mu$ M, suggesting that under those conditions  $\alpha$ -mangostin is well absorbed (25).

Multiple molecular pathways have been shown to be deregulated in PCa including the CDKs. These enzymes are responsible for promoting cell cycle progression and transcription of genes involved in cell replication and survival. It has been well established that early on in prostate carcinogenesis, a deregulation of CDKs/cyclins occurs leading to the phosphorylation of retinoblastoma proteins leading to an inability to regulate the cell cycle. One of the earlier events in carcinogenesis is the loss of cell cycle control (26) and would seem to be an ideal target for cancer chemoprevention. Another potential benefit of targeting these cell cycle regulatory targets is that cell cycle deregulation occurs over the full spectrum of cancers. Recently, investigators have begun to evaluate CDK inhibitors as chemopreventive agents and have been able to successfully show that CDK inhibitors are effective in preventing colon tumorigenesis in a mouse model (27). The results presented in this study suggest that  $\alpha$ -mangostin directly inhibits CDK4 as shown in cell-free biochemical kinase assays. Furthermore, using molecular modeling, we have generated hypothetical binding arrangements between CDK4 and  $\alpha$ -mangostin. It is tempting to speculate that  $\alpha$ -mangostin due to its flat/planar structure, hydrophobic isoprenyl groups, along with neighboring hydrogen-bonding donors at positions 1 and 3 are able to fit within the deep and narrow ATP binding pocket. Based on our analysis, it would seem that the isoprenyl groups may offer an advantage to other nonisoprenylated chemicals by encouraging interactions with amino acids deep within the hydrophobic molecular binding pocket. Furthermore, the isoprenyl groups may allow for flexible docking and subsequent better filling of the ATP binding pocket. It is important to note, based on our modeling, there still appears to be room to fill the pocket possibly affording an opportunity to further modify  $\alpha$ -mangostin in order to develop more effective CDK4 inhibitors. Alternatively, there may be other xanthones available as natural products from the mangosteen fruit that are better inhibitors of CDK4. Cocrystallization studies of  $\alpha$ -mangostin with CDK4 are needed to determine how  $\alpha$ -mangostin interacts with CDK4 and determine if it is a competitive inhibitor or an allosteric inhibitor of CDK4 or even a combination of the two. The retinoblastoma protein has up to 14 different phosphorylation sites and further analysis by mass spectrometry is needed to determine which phosphorylation sites are specifically inhibited. Once this inhibition profile is established a side-by-side comparison with other CDK4 inhibitors (i.e. xanthones and nonxanthones) is needed to identify any unique properties of  $\alpha$ -mangostin. Alternatively, there may be other xanthones that target pathways other than CDK4/cyclin D1/retinoblastoma encouraging a multitargeted strategy.

Previously,  $\alpha$ -mangostin has been shown to suppress JNK protein expression leading to an inhibition of matrix metalloproteinases-2/9 in PCa cells (18). We did not observe a strong direct effect of  $\alpha$ -mangostin directly inhibiting JNK kinase activity which taken together suggests that  $\alpha$ -mangostin may target proteins upstream of JNK. Several studies have reported the proapoptotic effects of  $\alpha$ -mangostin in colon and leukemia cell lines (24,28–30). This was in agreement with our analysis of PCa cells treated with  $\alpha$ -mangostin where we observed the activation of the caspase cascade followed by apoptosis in both PC3 and 22Rv1 cells after 24 and 48 h. Another interesting observation is that  $\alpha$ -mangostin appeared to be more effective at decreasing cell viability in LNCaP cells and 22Rv1 cells which have mutated receptors at T877A and H874Y, respectively. Based on these results, we are evaluating the targeting of androgen receptor with  $\alpha$ -mangostin.

In summary, the major finding of the present study is the demonstration that  $\alpha$ -mangostin, derived from the purple mangosteen fruit, inhibits CDK4 leading to a decrease in the phosphorylation of the retinoblastoma proteins leading to G<sub>1</sub> cell cycle arrest in 22Rv1PCa

cells at doses as low as 7.5  $\mu$ M after 24 h of treatment. Apoptosis was observed at 15  $\mu$ M after 48 h of treatment. This data suggests that lower sustained doses will promote cell cycle arrest, whereas higher doses have the potential to promote apoptosis, however further work is needed to characterize this. We observed that  $\alpha$ -mangostin significantly suppressed tumor formation in nude mice implanted with 22Rv1 cells. This is an important observation in that many patients diagnosed with PCa that are undergoing watchful waiting may be excellent candidates for chemopreventive agents that delay and slow the process of carcinogenesis. Together, these findings provide a more thorough molecular understanding to previous reports (24,28,29) of  $\alpha$ -mangostin decreasing cell viability and promoting G<sub>1</sub> cell cycle arrest. Given the evidence of  $\alpha$ -mangostin's anticancer activity, further work is needed to determine its potential as a chemotherapeutic and/or chemopreventive agent.

### Funding

Clinical and Translational Science Award (CTSA) KL2 program NIH 1KL2RR025012-01 and 1R03CA138953-01A1 (to J.J.J.); US PHS Grant T32AR055893 (to I.A.S.); NIEHS Grant T32ES007015 (to D.N.S.).

*Conflict of Interest Statement:* None declared.

### References

- Johnson, J.J. (2011) Carnosol: a promising anti-cancer and anti-inflammatory agent. *Cancer Lett.*, **305**, 1–7.
- Johnson, J.J. *et al.* (2010) Green tea polyphenols for prostate cancer chemoprevention: a translational perspective. *Phytomedicine*, **17**, 3–13.
- Johnson, J.J. *et al.* (2007) Curcumin for chemoprevention of colon cancer. *Cancer Lett.*, **255**, 170–181.
- Obolskiy, D. *et al.* (2009) *Garcinia mangostana* L.: a phytochemical and pharmacological review. *Phytother. Res.*, **23**, 1047–1065.
- Pedraza-Chaverri, J. *et al.* (2008) Medicinal properties of mangosteen (*Garcinia mangostana*). *Food Chem. Toxicol.*, **46**, 3227–3239.
- Chen, L.G. *et al.* (2008) Anti-inflammatory activity of mangostins from *Garcinia mangostana*. *Food Chem. Toxicol.*, **46**, 688–693.
- Chomnawang, M.T. *et al.* (2007) Effect of *Garcinia mangostana* on inflammation caused by *Propionibacterium acnes*. *Fitoterapia*, **78**, 401–408.
- Gopalakrishnan, C. *et al.* (1980) Effect of mangostin, a xanthone from *Garcinia mangostana* Linn. in immunopathological & inflammatory reactions. *Indian J. Exp. Biol.*, **18**, 843–846.
- Sundaram, B.M. *et al.* (1983) Antimicrobial activities of *Garcinia mangostana*. *Planta Med.*, **48**, 59–60.
- Devi Sampath, P. *et al.* (2007) Cardioprotective effect of alpha-mangostin, a xanthone derivative from mangosteen on tissue defense system against isoproterenol-induced myocardial infarction in rats. *J. Biochem. Mol. Toxicol.*, **21**, 336–339.
- Sampath, P.D. *et al.* (2008) Ameliorative prospective of alpha-mangostin, a xanthone derivative from *Garcinia mangostana* against beta-adrenergic catecholamine-induced myocardial toxicity and anomalous cardiac TNF- $\alpha$  and COX-2 expressions in rats. *Exp. Toxicol. Pathol.*, **60**, 357–364.
- Jung, H.A. *et al.* (2006) Antioxidant xanthenes from the pericarp of *Garcinia mangostana* (Mangosteen). *J. Agric. Food Chem.*, **54**, 2077–2082.
- Marquez-Valadez, B. *et al.* (2009) The natural xanthone alpha-mangostin reduces oxidative damage in rat brain tissue. *Nutr. Neurosci.*, **12**, 35–42.
- Pedraza-Chaverri, J. *et al.* (2009) ROS scavenging capacity and neuroprotective effect of alpha-mangostin against 3-nitropropionic acid in cerebellar granule neurons. *Exp. Toxicol. Pathol.*, **61**, 491–501.
- Weecharangan, W. *et al.* (2006) Antioxidative and neuroprotective activities of extracts from the fruit hull of mangosteen (*Garcinia mangostana* Linn.). *Med. Princ. Pract.*, **15**, 281–287.
- Williams, P. *et al.* (1995) Mangostin inhibits the oxidative modification of human low density lipoprotein. *Free Radic. Res.*, **23**, 175–184.
- Nabandith, V. *et al.* (2004) Inhibitory effects of crude alpha-mangostin, a xanthone derivative, on two different categories of colon preneoplastic lesions induced by 1, 2-dimethylhydrazine in the rat. *Asian Pac. J. Cancer Prev.*, **5**, 433–438.
- Hung, S.H. *et al.* (2009) Alpha-mangostin suppresses PC-3 human prostate carcinoma cell metastasis by inhibiting matrix metalloproteinase-2/9 and urokinase-plasminogen expression through the JNK signaling pathway. *J. Agric. Food Chem.*, **57**, 1291–1298.
- Suh, Y. *et al.* (2009) A plant flavonoid fisetin induces apoptosis in colon cancer cells by inhibition of COX2 and Wnt/EGFR/NF-kappaB-signaling pathways. *Carcinogenesis*, **30**, 300–307.
- Johnson, J.J. *et al.* (2008) Carnosol, a dietary diterpene, displays growth inhibitory effects in human prostate cancer PC3 cells leading to G<sub>2</sub>-phase cell cycle arrest and targets the 5'-AMP-activated protein kinase (AMPK) pathway. *Pharm. Res.*, **25**, 2125–2134.
- Johnson, J.J. *et al.* (2010) Disruption of androgen and estrogen receptor activity in prostate cancer by a novel dietary diterpene carnosol: implications for chemoprevention. *Cancer Prev. Res. (Phila.)*, **3**, 1112–1123.
- Day, P.J. *et al.* (2009) Crystal structure of human CDK4 in complex with a D-type cyclin. *Proc. Natl Acad. Sci. USA*, **106**, 4166–4170.
- Settheetham, W. *et al.* (1995) Study of genotoxic effects of antidiarrheal medicinal herbs on human cells *in vitro*. *Southeast Asian J. Trop. Med. Public Health*, **26** (suppl. 1), 306–310.
- Matsumoto, K. *et al.* (2003) Induction of apoptosis by xanthenes from mangosteen in human leukemia cell lines. *J. Nat. Prod.*, **66**, 1124–1127.
- Syamsudin, F. *et al.* (2009) HPLC analysis and pharmacokinetic study of mangostin after oral administration in rats. *Pharm. Res.*, **2**, 43–49.
- Syljuasen, R.G. *et al.* (1999) Loss of normal G<sub>1</sub> checkpoint control is an early step in carcinogenesis, independent of p53 status. *Cancer Res.*, **59**, 1008–1014.
- Boquoi, A. *et al.* (2009) Chemoprevention of mouse intestinal tumorigenesis by the cyclin-dependent kinase inhibitor SNS-032. *Cancer Prev. Res. (Phila.)*, **2**, 800–806.
- Matsumoto, K. *et al.* (2005) Xanthenes induce cell-cycle arrest and apoptosis in human colon cancer DLD-1 cells. *Bioorg. Med. Chem.*, **13**, 6064–6069.
- Matsumoto, K. *et al.* (2004) Preferential target is mitochondria in alpha-mangostin-induced apoptosis in human leukemia HL60 cells. *Bioorg. Med. Chem.*, **12**, 5799–5806.
- Menasria, F. *et al.* (2008) Apoptotic effects on B-cell chronic lymphocytic leukemia (B-CLL) cells of heterocyclic compounds isolated from Guttiferae. *Leuk. Res.*, **32**, 1914–1926.

Received December 9, 2010; revised November 23, 2011; accepted December 3, 2011